

Disentangle to Create: Structure-Level Disentangled Diffusion Model for Few-Shot Chinese Font Generation

Jie Li^{1,2}, Suorong Yang^{1,3*}, Jian Zhao⁴, and Furao Shen^{1,2*}

¹ State Key Laboratory for Novel Software Technology, Nanjing University, China

² School of Artificial Intelligence, Nanjing University, China

³ Department of Computer Science and Technology, Nanjing University, China

⁴ School of Electronic Science and Engineering, Nanjing University, China

Abstract. Few-shot Chinese font generation aims to synthesize new characters in a target style using only a handful of reference images. Achieving accurate content rendering and faithful style transfer requires effective disentanglement between content and style. However, existing approaches achieve only feature-level disentanglement, allowing the generator to re-entangle these features, leading to content distortion and degraded style fidelity. We propose the Structure-Level Disentangled Diffusion Model (SLD-Font), which receives content and style information from two separate channels. SimSun-style images are used as content templates and concatenated with noisy latent features as the input. Style features, extracted by a CLIP model from target-style images, are integrated through cross-attention. Additionally, we train a Background Noise Removal module in the pixel space to remove background noise in complex stroke regions. Based on theoretical validation of disentanglement effectiveness, we introduce a parameter-efficient fine-tuning strategy that updates only the style-related modules. This allows the model to better adapt to new styles while avoiding overfitting to the reference images' content. We further introduce the Grey and OCR metrics to evaluate the content quality of generated characters. Experimental results show that SLD-Font achieves significantly higher style fidelity while maintaining comparable content accuracy to existing state-of-the-art methods.

Keywords: Diffusion Models · Image Generation · Few-shot Chinese Font Generation

1 Introduction

Chinese font generation integrates linguistic expression with aesthetic design to support personalized branding, historical media authenticity, and digital restoration, promoting cultural creativity and artistic exploration in modern digital contexts [25, 40]. However, unlike English letters, Chinese characters have complex structures and exist in large quantities. The GB2312 standard includes 6,763

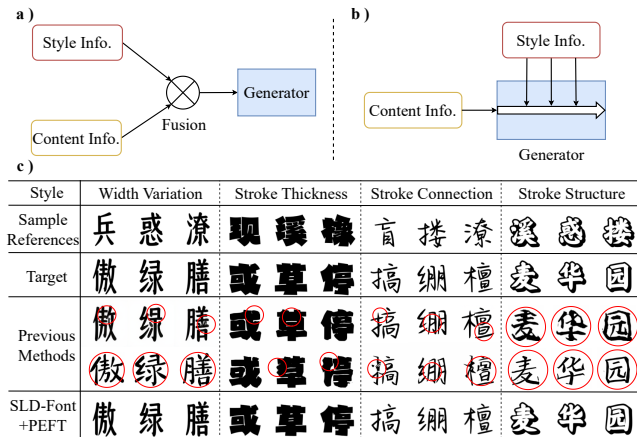


Fig. 1: Existing methods, as illustrated in (a), are typically built upon a framework that achieves feature-level disentanglement. In contrast, our approach achieves structure-level disentanglement as shown in (b), yielding more robust content preservation and style controllability. As demonstrated in (c), our method produces Chinese characters with noticeably higher visual quality.

commonly used characters, and the GB18030 standard covers over 27,000 [34,35]. As a result, manually designing Chinese fonts is extremely time-consuming and labor-intensive. To this end, deep generative models have been increasingly adopted to synthesize Chinese characters in novel styles with minimal reference samples [5, 11, 19, 23, 43]. Despite achieving promising results, they struggle to preserve content faithfully while maintaining high-quality style transfer.

Unlike style transfer [2, 3, 17], which focuses on transferring color and texture, font generation demands much higher content fidelity, as even slight deviations can lead to content errors. More importantly, the style of Chinese characters is typically conveyed through attributes, such as width, stroke thickness, connectivity, and structure, making content-style disentanglement a key determinant of visual quality and usability. Most existing methods are based on GANs [4, 19, 22, 23], or diffusion models [5, 11, 43]. They typically adopt separate encoders to extract content and style features, which are then fused and fed into the generator or injected into the U-Net [28] via cross-attention in Transformer blocks [39]. However, these approaches only perform disentanglement at the feature-level and lack explicit structure-level separation, leading to re-entanglement during generation. Consequently, as shown in Figure 1, such designs often produce Chinese characters with distorted structures or incomplete adaptation to the target style.

In this paper, we propose a **Structure-Level Disentangled Diffusion Model** for few-shot Chinese font generation (SLD-Font). As illustrated in Fig. 1(b), the generator is designed to process content information as its primary function, while being guided by style information throughout the generation process, thereby achieving structure-level disentanglement between content and style.

Specifically, we concatenate the SimSun-style source image as content information with the noise-corrupted image along the channel dimension [30] and feed the concatenated tensor into the U-Net. For style information, we extract features from each reference image by the CLIP image encoder [42], and inject them into the U-Net via cross-attention in a token-like manner. In this design, the U-Net backbone focuses on content representation, while style information modulates the generation process, enabling effective structural-level disentanglement. Following LDMs [27], we perform the diffusion process in the latent space of a VAE [38]. Considering that the VAE tends to introduce noise and artifacts [18, 26, 36], we further adopt a pixel-space Background Noise Removal (BNR) module to refine the outputs and improve the content fidelity. By disentangling content and style at the structure level, our method isolates the style-related parameters, enabling parameter-efficient fine-tuning (PEFT) [6, 10, 15]. This allows the model to adapt to the target style with minimal updates, avoiding overfitting to content patterns, which is often seen in full fine-tuning, and making SLD-Font well-suited for few-shot scenarios.

Experimental results show that our proposed method outperforms existing methods across widely used evaluation metrics, such as ℓ_1 loss and Structural Similarity Index (SSIM) [41], demonstrating strong performance in both visual quality and content accuracy. To further evaluate the stringent structural and semantic requirements of font generation, we introduce two tailored evaluation metrics: Grey, which quantifies background noise through grayscale histogram comparison, and an OCR-based accuracy metric for content recognition. Even under these more challenging evaluations, SLD-font achieves superior style consistency and precise content generation. In summary, our main contributions are as follows:

- We propose SLD-Font, in which content information is directly fed into the U-Net, and style information is incorporated via cross-attention, improving content and style fidelity through structure-level disentanglement.
- To mitigate artifacts introduced by the VAE, particularly in regions with complex strokes, we design a Background Noise Removal (BNR) module that operates in pixel space to suppress such noise in generated images.
- To the best of our knowledge, we are the first to introduce PEFT into few-shot font generation based on structure-level disentanglement. Theoretically and experimentally, fine-tuning on a few reference images enables more accurate style capture while mitigating content overfitting.
- In addition to traditional evaluation metrics, we further introduce two content-level indicators, Grey and OCR. Compared with SOTA methods using various metrics, our approach achieves much higher style similarity while maintaining comparable content accuracy.

2 Related Work

Font generation has evolved from manual design to automatic image synthesis using deep generative models. Early methods focused on single style transfer

with fully supervised learning, but these approaches were not scalable to large character sets [16, 40]. Recent advances have shifted towards few-shot font generation (FFG), which aims to synthesize new fonts from a limited number of reference images by disentangling style and content representations. Early methods used VAEs [18, 26], whereas current methods are mainly based on GAN [9] and diffusion [14, 32, 33].

VAE-based methods attempt to model content-style separation in latent space. SA-VAE [36] introduces a pair-wise optimization strategy to enable style inference from only one or few reference samples. EMD [45] proposes an architecture composed of style and content encoders, allowing transfer to unseen styles and contents. GAN-based models typically fuse content and style in a single generative stream. AGISNet [8] utilizes two collaboratively working decoders to generate the glyph shape simultaneously. MX-Font [23] innovates by employing multiple localized experts to automatically extract diverse local styles, while LF-Font [22] introduces a low-rank factorization mechanism to decompose style into component and style factors. NTF [4] treats font generation as a continuous transformation task using a neural transformation field. CG-GAN [19] brings a new perspective by using a Component-Aware Module to provide fine-grained supervision. Fs-Font [37] enhances local accuracy with a cross-attention mechanism that aligns spatial regions in content images with corresponding local styles in the references. Diffusion-based methods have recently emerged as a promising alternative due to their stable training and superior visual fidelity. Diff-Font [11] is the first to apply diffusion models to FFG, leveraging component-level conditions such as strokes or radicals. FontDiffuser [43] introduces multi-scale content aggregation and a style contrastive refinement module to improve local detail preservation. MSD-Font [5] decomposes the generation process into three stages: structure generation, style transfer, and refinement—mimicking human workflows. HFH-Font [21] further improves visual resolution and vectorization quality through component-aware conditioning. However, none of these methods achieve explicit structure-level content–style disentanglement, which is critical for maintaining character integrity and ensuring controllable style transfer.

3 Methodology

As shown in Figure 2, we propose SLD-Font, a Structure-level Disentangled Diffusion Model for efficient few-shot Chinese font generation. Built upon the Latent Diffusion Model (LDM) framework, SLD-Font separates content and style information through distinct pathways to achieve effective disentanglement. A Background Noise Removal (BNR) module is introduced at the pixel level to correct errors caused by latent–pixel conversion. Leveraging this disentanglement, we further adopt parameter-efficient fine-tuning to improve adaptability to unseen styles.

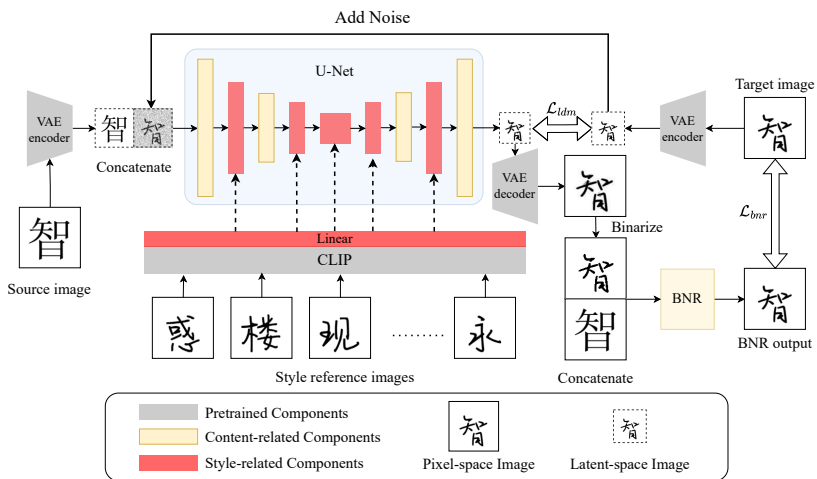


Fig. 2: Both source and target images are encoded into the latent space through a VAE encoder. Gaussian noise is added to the latent target representation during diffusion, producing a noisy latent image that is concatenated with the source and fed into the U-Net. Content and style are disentangled within the U-Net: content components capture structural patterns from the source image, while style components receive CLIP-extracted features from multiple style reference images and inject them via cross-attention. The U-Net output is decoded by the VAE, binarized, and refined in pixel space using the BNR module to produce clean and accurate glyphs.

3.1 Preliminaries on Latent Diffusion Models

A diffusion model learns to generate data by reversing the gradual noising process, step by step transforming random noise back into structured data [14, 33]. SLD-Font is built upon the LDMs [27], which significantly reduce computational cost by performing the diffusion process in a compressed VAE [36, 38] latent space while preserving high-quality generation. Given an image x in pixel space, it is first encoded into latent space by the VAE encoder as $z_0 = \mathcal{E}(x)$. The forward process progressively adds noise to z_0 until its distribution approaches a standard Gaussian distribution $z_T \sim \mathcal{N}(\mathbf{0}, \mathbf{I})$:

$$z_t = \sqrt{\alpha_t} z_{t-1} + \sqrt{1 - \alpha_t} \varepsilon, \quad \varepsilon \sim \mathcal{N}(\mathbf{0}, \mathbf{I}), \quad (1)$$

$$z_t = \sqrt{\bar{\alpha}_t} z_0 + \sqrt{1 - \bar{\alpha}_t} \varepsilon, \quad \varepsilon \sim \mathcal{N}(\mathbf{0}, \mathbf{I}), \quad (2)$$

where α_t is a time-dependent hyperparameter, $\bar{\alpha}_t = \prod_{i=1}^t \alpha_i$ and $t \in \{1, 2, \dots, T\}$, with T denoting the total number of diffusion steps.

The reverse process starts by sampling pure noise $z_T \sim \mathcal{N}(\mathbf{0}, \mathbf{I})$ and gradually denoises it to obtain z_0 . Each step from z_t to z_{t-1} is conditioned on z_0 and

calculated as:

$$q(z_{t-1} | z_t, z_0) = \mathcal{N}(z_{t-1}; \tilde{\mu}_t(z_t, z_0), \tilde{\beta}_t \mathbf{I}), \quad (3)$$

$$\tilde{\mu}_t(z_t, z_0) := \frac{\sqrt{\bar{\alpha}_{t-1}}(1 - \alpha_t)}{1 - \bar{\alpha}_t} z_0 + \frac{\sqrt{\bar{\alpha}_t}(1 - \bar{\alpha}_{t-1})}{1 - \bar{\alpha}_t} z_t, \tilde{\beta}_t := \frac{1 - \bar{\alpha}_{t-1}}{1 - \bar{\alpha}_t} (1 - \alpha_t), \quad (4)$$

The latent variable z_0 is then passed through the VAE decoder \mathcal{D} to obtain the reconstructed image in pixel space, denoted as $x = \mathcal{D}(z_0)$.

To implement the reverse process described in Eq. (3), LDMs use the U-Net model \hat{z}_θ to predict z_0 gradually. Following [5, 29], we adopt the strategy of directly predicting z_0 , rather than predicting noise as in the original DDPMs [14]. Noise prediction improves diversity, whereas directly predicting z_0 ensures a more deterministic process that better preserves content consistency in font generation. Given conditioning input c , the training objective of LDMs at time step t is defined as:

$$\mathcal{L}_{ldm} = \mathbb{E}_{t,x,\varepsilon} [\|z_0 - \hat{z}_\theta(z_t, c)\|_2^2], \quad (5)$$

The U-Net receives and processes conditioning information via cross-attention in transformer blocks [39].

3.2 Structure-Level Disentangled Diffusion Model

SLD-Font achieves structure-level disentanglement by introducing content and style information through two distinct pathways within the U-Net architecture. We formulate few-shot font generation as an image-to-image translation task conditioned on few reference images in the target style, aiming to transform source font images into the target style while preserving content accuracy. SimSun is selected as the source font due to its wide availability across devices and its clear and well-defined character structure. Given a character pair (x, y) , where x is the SimSun character and y is its corresponding character in the target style, we also provide a set of N target-style reference images r_1, r_2, \dots, r_N to provide style information. The overall framework of SLD-Font is illustrated in Figure 2.

For content information, a pre-trained VAE encoder is used to encode x and y into the latent space, resulting in z_x and the initial latent distribution z_y^0 . During training, we sample a time step $t \sim \text{Uniform}(1, \dots, T)$ and add noise to z_y^0 following Eq. (2):

$$z_y^t = \sqrt{\bar{\alpha}_t} z_y^0 + \sqrt{1 - \bar{\alpha}_t} \varepsilon, \quad \varepsilon \sim \mathcal{N}(\mathbf{0}, \mathbf{I}), \quad (6)$$

Following [30], we concatenate the SimSun-style content image z_x and the noisy target image z_y^t along the channel dimension as the input to the U-Net. The content image of a Chinese character clearly preserves its structural information. Using it as a template provides sufficient guidance for generating structurally accurate results.

For style information, we use a pre-trained CLIP model [42] to extract the style representation from each reference image, denoted as $s_i = \text{CLIP}(r_i)$. This

results in a style matrix $s \in \mathbb{R}^{N \times d}$, where d is the dimensionality of the style embedding. The style features s are injected into the U-Net through cross-attention in transformer blocks, allowing style conditioning during generation. This process resembles text prompts in text-to-image generation, except that our CLIP model treats all reference images equally, making the order of reference images irrelevant. Given the misalignment between CLIP’s pretraining objective and font generation [24, 42], we retrain the final projection layer to retain general visual representations while adapting to our task.

We adopt the strategy of predicting z_0 , and the loss function is defined as:

$$\hat{z}_y^0 = \hat{z}_\theta(\text{concat}(z_y^t, z_x), s), \quad (7)$$

$$\mathcal{L}_{ldm} = \mathbb{E}_{t,(x,y),\{r_1,r_2,\dots,r_N\},\varepsilon} [\|z_y^0 - \hat{z}_y^0\|_2^2], \quad (8)$$

Let $\theta = \theta_c \cup \theta_s$ denote the model parameters, corresponding to the content and style pathways highlighted in yellow and red in Figure 2, respectively. Content-related θ_c serves as the backbone for processing content spatial patterns, and θ_s adjusts channel expression through style modulation by cross-attention. This division of roles forms the basis of disentanglement. By isolating content and style through distinct input paths and attention mechanisms, SLD-Font achieves effective content-style disentanglement, enabling accurate content preservation and flexible style transfer.

3.3 Background Noise Removal Module

Since Latent Diffusion Models rely on a VAE to transform between latent and pixel spaces, they inevitably introduce some noise during decoding [18, 26, 38], as shown in the supplemental material. In regular text-to-image tasks, the noise is often masked by rich color. However, it becomes visible in font generation, especially around dense strokes on clean backgrounds. As illustrated in Figure 3, noise artifacts can be clearly observed in the densely stroked right part of the character “Ye” when directly decoded from the VAE. This noise is reflected in the grayscale distribution: in the target image, pixel intensities are concentrated near 0 and 1, with only a small proportion of intermediate gray values. In contrast, the VAE output shows a significant accumulation of pixels near 1, corresponding to the undesired noise regions.

We propose the Background Noise Removal (BNR) module to address the background noise present in generated Chinese characters. As shown in Figure 3, although some noise exists, the overall grayscale tendency of the VAE output remains largely correct. Based on this observation, we convert the decoded image into a binary image and concatenate it with the SimSun source image x along the channel dimension. This combined input is then fed into the BNR module. The BNR module is implemented as a U-Net and outputs a noise-removed image:

$$\tilde{y} = \text{BNR}(\text{Binarize}(\text{concat}(\mathcal{D}(\hat{z}_y^0)), x)), \quad (9)$$

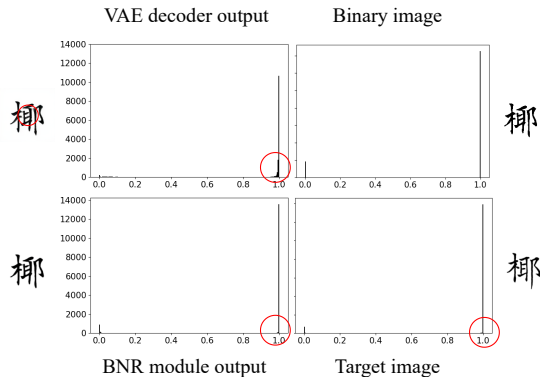


Fig. 3: The VAE output shows background noise in dense stroke areas, which is visible in the grayscale histogram. The BNR module effectively removes the noise.

Since the BNR module is trained in pixel space, it allows us to incorporate edge and perceptual losses that are not feasible in latent space. Specifically, we apply a Sobel-based edge loss [7] and a VGG perceptual loss [31] for better stroke sharpness and visual quality. The overall loss function is defined as:

$$\mathcal{L}_{bnr} = \ell_1(\tilde{y}, y) + \lambda_1 \ell_1(\text{Sobel}(\tilde{y}), \text{Sobel}(y)) + \lambda_2 \text{VGG}(\tilde{y}, y), \quad (10)$$

This setup enables the BNR module to effectively reduce background artifacts while preserving the content integrity of the generated characters. We train the BNR module based on the trained SLD-Font. It is worth noting that our SLD-Font adopts a training strategy that predicts z_y^0 , which means that at each diffusion time step, we can obtain an estimate of \hat{z}_y^0 using Eq. (7). For clarity, we refer to SLD-Font as the default version with the BNR module.

3.4 Parameter Efficient Fine-Tuning

Model can better adapt to the target task or data distribution by fine-tuning with a small number of task-specific samples, thereby improving performance and generation quality [10, 29]. However, in the few-shot font generation, the available data for fine-tuning is limited to only few reference style images. Direct fine-tuning under such constraints can lead to overfitting. Although the model may better adapt to the style pattern, allowing it to generate images that closely match the target style, it also overfits to the content patterns of the reference characters, resulting in content distortions, especially when generating unseen characters.

Theoretically Analysis SLD-Font employs structure-level disentanglement. The style information is injected into the U-Net through cross-attention mech-

anism, calculated as:

$$Q = W_Q h(z_y^t, z_x), K = W_K s, V = W_V s,$$

$$T = \frac{QK^\top}{\sqrt{d}}, A = \text{softmax}(T), O = AV, \mathcal{L} = \mathcal{L}(O),$$

where h denotes modules before the cross-attention layer, s represents style information extracted by CLIP, W_Q , W_K , and W_V are the projection matrices for the query, key, and value, respectively, d is the dimensionality of the hidden states, and \mathcal{L} represents the loss function associated with this layer. Gradients of the content and style conditions are:

$$G = \frac{\partial \mathcal{L}}{\partial O}, J_{\text{softmax}}(A) = \text{diag}(A) - AA^\top$$

$$\frac{\partial \mathcal{L}}{\partial z_x} = \left(\frac{\partial h}{\partial z_x} \right)^\top W_Q^\top \frac{1}{\sqrt{d}} J_{\text{softmax}}^\top(GV^\top) K, \quad (11)$$

$$\frac{\partial \mathcal{L}}{\partial s} = \frac{1}{\sqrt{d}} W_K^\top \left(J_{\text{softmax}}^\top(GV^\top) \right)^\top Q + W_V^\top A^\top G, \quad (12)$$

The optimization of the content channel z_x involves K and V , since the attention mechanism couples the content query Q with the style key K and value V through the softmax operation. However, K and V serve only as weighting terms during backpropagation, influencing the updates of parameters such as W_Q and h , while the parameters associated with K and V themselves remain unchanged. Similarly, the optimization of the style channel s depends on Q only through attention weights. Therefore, gradient propagation preserves the disentanglement between content and style. When we fine-tune only style-related parameters, the content information participates in optimization but does not affect content-related parameters.

We further conducted a gradient analysis under three experimental settings: Seen Chars Seen Font (SCSF), Unseen Chars Seen Font (UCSF), and Seen Chars Unseen Font (SCUF) based on the model trained in Section 3.2. We compute the gradients of all parameters within a batch of 128 samples under each of the three settings. We categorize the parameters into four groups: (1) K and V projection matrix in Cross-Attention modules (KV), (2) Transformer Blocks (Trans_block), (3) the last layer of CLIP (Clip), and (4) other parameters corresponding to content-related components (Others). It is worth noting that although the KV are part of the Trans_blocks, they directly receive style information and are therefore analyzed separately. Taking SCSF as the baseline, we evaluate the sensitivity of each parameter to content and style variations. For a given parameter x , let its magnitude of gradient under the SCSF setting be denoted as $G(x)$, and its magnitude of gradient under other settings as $G_*(x)$. We define their ratio $G_*(x)/G(x)$ as the parameter sensitivity metric, and report the mean sensitivity across each parameter group. The results are shown in Figure 4. Overall, the model exhibits higher sensitivity to unseen styles than to unseen characters. KV, Trans_block, and Clip exhibit higher sensitivity than

Others to unseen styles in SCUF. Clip and KV show greater responses as they directly encode and propagate style information, whereas the Trans_block plays a more auxiliary role in style adaptation. In contrast, for unseen characters in UCSF, the content-related components display higher sensitivity. At the same time, the Clip module shows a marked decrease in gradient magnitude compared with the unseen-style condition.

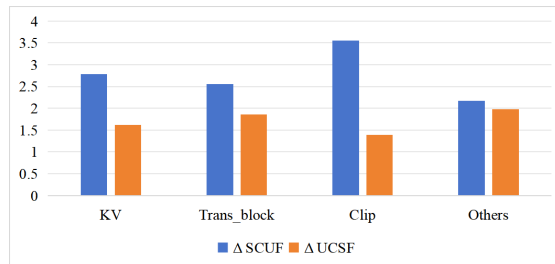


Fig. 4: Results of gradient analysis. Style-related parameters are more sensitive to unseen styles, while content-related parameters are more sensitive to unseen content.

Based on this observation, we treat all parameters that are more sensitive to style, including the Transformer blocks and the last layer of CLIP, as style-related parameters θ_s , and other parameters as content-related θ_c . We adopt a parameter-efficient fine-tuning strategy (PEFT) [6, 20, 29], where only the style-related components θ_s are updated, while the content-related θ_c are frozen. This enables the model to better adapt to the target style while preserving the content structure. Given the limited number of reference images, we aim to construct as many training pairs as possible. Given $N > 1$ reference images, we randomly select one as the target and choose subsets from the remaining $N - 1$ as reference inputs, resulting in $2^{N-1} - 1$ possible combinations. Thus, a total of $N(2^{N-1} - 1)$ unique training pairs can be constructed. During inference, we use all N reference images to guide generation.

4 Experiment

4.1 Experimental Settings

Implementation Details. Closely following the implementation settings of [5], all font images are resized to $128 \times 128 \times 3$, and the default number of reference images for few-shot generation is set to 8. The total number of diffusion steps is $T = 1000$. During training, each data sample consists of one SimSun source character image, one corresponding target-style character image, and 8 randomly selected non-target character images in the same target style as reference. The weights in Eq. (10) are set as $\lambda_1 = 1$ and $\lambda_2 = 0.05$. During fine-tuning, we train

Table 1: Quantitative comparison under SCUF and UCUF settings across diverse evaluation metrics. Since Font-diff only supports SCUF, we do not report the results under UCUF. **SCSF**: Seen Chars Seen Font. **UCUF**: Unseen Chars Seen Font.

Model	SCUF						UCUF					
	SSIM ↑	LPIPS ↓	FID ↓	L1 ↓	Grey ↑	OCR ↑	SSIM ↑	LPIPS ↓	FID ↓	L1 ↓	Grey ↑	OCR ↑
LF	0.307	0.275	1.275	0.255	0.381	0.986	0.304	0.283	1.298	0.257	0.380	0.978
MX	0.319	0.256	0.671	0.249	0.285	1.000	0.321	0.259	0.689	0.246	0.283	0.999
NTF	0.359	0.250	0.623	0.229	0.376	0.997	0.352	0.257	0.631	0.232	0.373	0.995
Font-diff (1shot)	0.298	0.270	4.087	0.254	0.518	0.949	-	-	-	-	-	-
FontDiffuser (1shot)	0.347	0.265	2.770	0.237	0.984	1.000	0.341	0.270	2.621	0.240	0.983	0.999
MSDFont	0.407	0.225	3.797	0.212	0.307	0.965	0.337	0.259	3.915	0.237	0.263	0.915
MSDFont+FT	0.433	0.208	3.438	0.197	0.447	0.940	0.337	0.259	4.210	0.233	0.366	0.857
SLD-Font (1shot)	0.381	0.231	1.718	0.227	0.990	0.999	0.352	0.245	1.734	0.239	0.990	0.998
SLD-Font	0.452	0.202	0.997	0.199	0.995	0.996	0.394	0.224	1.010	0.219	0.995	0.994
SLD-Font+PEFT	0.505	0.175	0.521	0.171	0.998	0.991	0.436	0.202	0.558	0.196	0.997	0.989

the model separately for each font style for 80 epochs and report the results by averaging the evaluation metrics across all fonts.

Datasets. Following prior works [5, 11], we collect 900 Chinese font styles from the Founder Type library, 840 for training (Seen Fonts) and the other 60 for evaluation (Unseen Fonts). During training, we randomly sample 800 Chinese characters from each seen font as the training set. For testing, 200 characters are randomly selected from the training set as seen content (Seen Chars), and another 200 unseen characters as unseen content (Unseen Chars). We evaluate in two scenarios: Seen Chars with Unseen Fonts (SCUF) and Unseen Chars with Unseen Fonts (UCUF).

Evaluation Metrics. We evaluate our method from both style and content perspectives. For style evaluation, we use several metrics: pixel-wise L1 loss, SSIM [41] for structural similarity, LPIPS [44] for perceptual quality, and FID [13] to assess distribution-level similarity. For content, inspired by Figure 3, we introduce a metric, Grey, which computes the cosine similarity between the grayscale histograms of the generated and target images to reflect background noise and structural consistency. We evaluate character correctness using pretrained PaddleOCR [1] and a ResNet-based OCR model [12] trained on our dataset. A character is considered correct if recognized by either model.

4.2 Comparison with State-of-the-arts

We compare SLD-Font with various methods, including MX [23], LF [22], NTF [4], Font-diff [11], FontDiffuser [43], and MSDFont [5]. FontDiffuser and Font-diff are one-shot methods. We also evaluate SLD-Font in the one-shot setting without retraining by randomly selecting a reference image as input. It is worth noting that MSDFont, an LDM-based approach, integrates the concatenated features from the structure and style encoders into the U-Net through cross-attention. For fairness, all methods are evaluated using the same settings.

As shown in Table 1, under both settings, SLD-Font consistently achieves the best performance compared to other methods. This shows that our method

can generate characters closer to the ground truth, with better perceptual quality and stronger preservation of character structure. Building on structure-level disentanglement, the parameter-efficient fine-tuned version, SLD-Font+PEFT, greatly improves style consistency, achieving the best performance across all style metrics. For content-related metrics, Grey reaches 0.998, and OCR remains high at 0.991. Although content performance shows a slight decline, style-related performance improves significantly. This demonstrates that our parameter-efficient strategy successfully adapts to new styles while largely preserving content integrity, validating the benefit of structure-level disentanglement. Under the UCUF setting, results are similar to those observed in SCUF, with SLD-Font+PEFT achieving superior overall performance compared to existing approaches. Since PEFT only optimizes style information and lacks adaptation to content, the improvement is less significant than in the SCUF setting. For comparison, we also fine-tune MSDFont (MSDFont+FT). In the SCUF setting, although MSD-Font+FT shows improved style metrics, its content performance drops. In the UCUF setting, the overall performance even degrades, highlighting the importance of structure-level content–style disentanglement, especially OCR, indicating that the model has overfitted to the content.

4.3 Visualization Analysis

Scenario	SCUF						UCUF					
Sample Ref	惑	惑	惑	惑	惑	惑	惑	惑	惑	惑	惑	惑
LF	性	檬	泥	积	氮	淋	蜻	春	唯	滋	邑	洗
MX	性	檬	泥	积	氮	淋	蜻	春	唯	滋	邑	洗
NTF	性	檬	泥	积	氮	淋	蜻	春	唯	滋	邑	洗
FontDiffuser	性	檬	泥	积	氮	淋	蜻	春	唯	滋	邑	洗
Font-diff	性	檬	泥	积	氮	淋	蜻	春	唯	滋	邑	洗
MSDFont	性	檬	泥	积	氮	淋	蜻	春	唯	滋	邑	洗
SLD-Font	性	檬	泥	积	氮	淋	蜻	春	唯	滋	邑	洗
SLD-Font+PEFT	性	檬	泥	积	氮	淋	蜻	春	唯	滋	邑	洗
Target	性	檬	泥	积	氮	淋	蜻	春	唯	滋	邑	洗
Style	Simple Cases	Width Variation	Stroke Thickness	Stroke Connection	Stroke Structure	Hard Cases	Simple Cases	Width Variation	Stroke Thickness	Stroke Connection	Stroke Structure	Hard Cases

Fig. 5: Visualization of Chinese character generation results under SCUF and UCUF settings, illustrating two fonts for each of six representative style characteristics. Problematic generations are highlighted with red circles.

To better understand the effectiveness of our method, we visualize the generation results in Figure 5. It can be seen that all models accurately capture both the content and style of the target font, while LF and MX show background noise artifacts. FontDiffuser fails to handle narrow-width fonts, while SLD-Font struggles with flat-shaped fonts. However, after applying PEFT, the generated fonts closely match the target style. Although all methods perform well on thin

fonts, LF, NTF, FontDiffuser, and Font-diff exhibit noise in complex stroke regions when generating thicker fonts. In terms of stroke connection, only SLD-Font+PEFT successfully reproduces the correct connectivity consistent with the target font. Regarding stroke structure, the rightmost example shows a font with shadowed strokes. Font-diff captures the stylistic shadowing but fails to produce the correct image. SLD-Font generates the correct character structure, though the shadow effect is less pronounced. SLD-Font+PEFT achieves the best balance, accurately preserving both structure and stylistic detail. Hard cases involve semi-cursive and cursive scripts, which inherently deviate from standard stroke structures. Most baseline methods prioritize structural fidelity, thereby failing to imitate the target style closely. SLD-Font+PEFT generates outputs that best resemble the style of the reference.



Fig. 6: Visualization of handwritten style test.

We have evaluated SLD-Font’s performance on 60 unseen typefaces. However, all of these are printed fonts, which are generally simpler in style compared to handwritten ones. Handwritten fonts exhibit higher variability, posing a greater challenge for accurate style adaptation. In this section, we use handwritten characters as references and evaluate the model on both seen and unseen characters. As shown in Figure 6, the results demonstrate that SLD-Font+PEFT effectively captures the reference style, producing characters visually consistent with the handwritten examples, which indicates strong style fitting capability.

4.4 Efficiency Analysis

We calculate the time required for fine-tuning to a single font style. As shown in Table 2, although the fine-tuning strategies differ substantially in design and the amount of trainable parameters, their actual fine-tuning times remain surprisingly close. This is because the major computational cost lies in data processing and latent encoding rather than parameter updates. Therefore, the time costs of our method remain at a low level.

Table 2: Comparison of different fine-tuning strategies in terms of parameter size and fine-tuning time for a single font style. Experiments are conducted on a single NVIDIA V100 GPU.

Strategy	CLIP	KV	ALL	PEFT
Num. Trainable	0.79M	2.36M	34.67M	7.30M
Time (s)	116.99	120.97	126.9	121.66

4.5 Ablation Study

In this section, we conduct ablation studies on SLD-Font, focusing on the BNR module and fine-tuning mechanism. The experiments are carried out under the UCUF setting. Ablation results are presented in Table 3.

Table 3: Effect of the component in our method. “CLIP” tunes the last CLIP layer, “KV” the K/V projections, “ALL” all parameters, and “PEFT” applies parameter-efficient fine-tuning.

Strategy	BNR	SSIM \uparrow	LPIPS \downarrow	Fid \downarrow	L1 \downarrow	Grey \uparrow	OCR \uparrow
No	\times	0.377	0.222	2.189	0.220	0.896	0.993
CLIP	\times	0.376	0.222	2.187	0.220	0.896	0.992
KV	\times	0.390	0.214	1.781	0.212	0.898	0.994
ALL	\times	0.388	0.210	2.164	0.210	0.510	0.973
PEFT	\times	0.423	0.202	1.719	0.196	0.779	0.986
No	\checkmark	0.394	0.224	1.010	0.219	0.995	0.994
CLIP	\checkmark	0.395	0.224	1.035	0.219	0.995	0.994
KV	\checkmark	0.410	0.217	0.735	0.211	0.997	0.996
ALL	\checkmark	0.405	0.215	0.642	0.208	0.997	0.984
PEFT	\checkmark	0.436	0.202	0.558	0.196	0.997	0.989

The BNR module brings clear improvements in content quality by effectively removing noise from the original images and mitigating the content degradation caused by fine-tuning. As a result of improved content consistency, most style metrics have improved as well.

We compare four fine-tuning strategies: updating the last CLIP layer, adjusting K/V projections in cross-attention, tuning all parameters, and parameter-efficient fine-tuning that updates style-related components. The CLIP strategy yields only minor gains over the baseline, indicating that improvements at the feature level remain limited. In contrast, KV, ALL, and PEFT markedly improve stylization quality. KV achieves moderate style enhancement with minimal content degradation, while ALL and PEFT introduce varying degrees of content loss, with ALL exhibiting a greater loss but fewer improvements in style. By freezing content-related parameters, PEFT preserves strong content fidelity while sig-

nificantly boosting style performance, making it the most effective strategy in few-shot scenarios.

5 Conclusion

In this paper, we introduce SLD-Font, a structure-level disentangled diffusion model for few-shot Chinese font generation. By separating content and style pathways within the generator and integrating CLIP-based style guidance, our model achieves effective structure-level disentanglement. To further enhance visual clarity, a BNR module is introduced. Meanwhile, a parameter-efficient fine-tuning strategy enables rapid adaptation to new styles without overfitting to content patterns of reference images in few-shot setting. Extensive experiments demonstrate that SLD-Font preserves content integrity and significantly improves style fidelity over existing diffusion-based methods.

References

1. Authors, P.: Paddleocr, awesome multilingual ocr toolkits based on paddlepaddle. <https://github.com/PaddlePaddle/PaddleOCR> (2020)
2. Chung, J., Hyun, S., Heo, J.P.: Style injection in diffusion: A training-free approach for adapting large-scale diffusion models for style transfer. In: Proceedings of the IEEE/CVF conference on computer vision and pattern recognition. pp. 8795–8805 (2024)
3. Chung, J., Hyun, S., Heo, J.P.: Style injection in diffusion: A training-free approach for adapting large-scale diffusion models for style transfer. In: Proceedings of the IEEE/CVF conference on computer vision and pattern recognition. pp. 8795–8805 (2024)
4. Fu, B., He, J., Wang, J., Qiao, Y.: Neural transformation fields for arbitrary-styled font generation. In: Proceedings of the IEEE/CVF conference on computer vision and pattern recognition. pp. 22438–22447 (2023)
5. Fu, B., Yu, F., Liu, A., Wang, Z., Wen, J., He, J., Qiao, Y.: Generate like experts: Multi-stage font generation by incorporating font transfer process into diffusion models. In: Proceedings of the IEEE/CVF Conference on Computer Vision and Pattern Recognition. pp. 6892–6901 (2024)
6. Fu, Z., Yang, H., So, A.M.C., Lam, W., Bing, L., Collier, N.: On the effectiveness of parameter-efficient fine-tuning. In: Proceedings of the AAAI conference on artificial intelligence. vol. 37, pp. 12799–12807 (2023)
7. Gao, W., Zhang, X., Yang, L., Liu, H.: An improved sobel edge detection. In: 2010 3rd International conference on computer science and information technology. vol. 5, pp. 67–71. IEEE (2010)
8. Gao, Y., Guo, Y., Lian, Z., Tang, Y., Xiao, J.: Artistic glyph image synthesis via one-stage few-shot learning. *ACM Transactions on Graphics (ToG)* **38**(6), 1–12 (2019)
9. Goodfellow, I.J., Pouget-Abadie, J., Mirza, M., Xu, B., Warde-Farley, D., Ozair, S., Courville, A., Bengio, Y.: Generative adversarial nets. *Advances in neural information processing systems* **27** (2014)
10. Han, Z., Gao, C., Liu, J., Zhang, J., Zhang, S.Q.: Parameter-efficient fine-tuning for large models: A comprehensive survey. *Transactions on Machine Learning Research* **2024** (2024)
11. He, H., Chen, X., Wang, C., Liu, J., Du, B., Tao, D., Yu, Q.: Diff-font: Diffusion model for robust one-shot font generation. *International Journal of Computer Vision* **132**(11), 5372–5386 (2024)
12. He, K., Zhang, X., Ren, S., Sun, J.: Deep residual learning for image recognition. In: Proceedings of the IEEE conference on computer vision and pattern recognition. pp. 770–778 (2016)
13. Heusel, M., Ramsauer, H., Unterthiner, T., Nessler, B., Hochreiter, S.: Gans trained by a two time-scale update rule converge to a local nash equilibrium. *Advances in neural information processing systems* **30** (2017)
14. Ho, J., Jain, A., Abbeel, P.: Denoising diffusion probabilistic models. *Advances in neural information processing systems* **33**, 6840–6851 (2020)
15. Hounsby, N., Giurgiu, A., Jastrzebski, S., Morrone, B., De Laroussilhe, Q., Gesmundo, A., Attariyan, M., Gelly, S.: Parameter-efficient transfer learning for nlp. In: International conference on machine learning. pp. 2790–2799. PMLR (2019)
16. Isola, P., Zhu, J.Y., Zhou, T., Efros, A.A.: Image-to-image translation with conditional adversarial networks. In: Proceedings of the IEEE conference on computer vision and pattern recognition. pp. 1125–1134 (2017)

17. Jeong, J., Kwon, M., Uh, Y.: Training-free style transfer emerges from h-space in diffusion models. arXiv preprint arXiv:2303.15403 **3**(1), 2 (2023)
18. Kingma, D.P., Welling, M.: Auto-encoding variational bayes. arXiv preprint arXiv:1312.6114 (2013)
19. Kong, Y., Luo, C., Ma, W., Zhu, Q., Zhu, S., Yuan, N., Jin, L.: Look closer to supervise better: One-shot font generation via component-based discriminator. In: Proceedings of the IEEE/CVF conference on computer vision and pattern recognition. pp. 13482–13491 (2022)
20. Kumari, N., Zhang, B., Zhang, R., Shechtman, E., Zhu, J.Y.: Multi-concept customization of text-to-image diffusion. In: Proceedings of the IEEE/CVF conference on computer vision and pattern recognition. pp. 1931–1941 (2023)
21. Li, H., Lian, Z.: Hfh-font: Few-shot chinese font synthesis with higher quality, faster speed, and higher resolution. ACM Transactions on Graphics (TOG) **43**(6), 1–16 (2024)
22. Park, S., Chun, S., Cha, J., Lee, B., Shim, H.: Few-shot font generation with localized style representations and factorization. In: Proceedings of the AAAI conference on artificial intelligence. vol. 35, pp. 2393–2402 (2021)
23. Park, S., Chun, S., Cha, J., Lee, B., Shim, H.: Multiple heads are better than one: Few-shot font generation with multiple localized experts. In: Proceedings of the IEEE/CVF international conference on computer vision. pp. 13900–13909 (2021)
24. Radford, A., Kim, J.W., Hallacy, C., Ramesh, A., Goh, G., Agarwal, S., Sastry, G., Askell, A., Mishkin, P., Clark, J., et al.: Learning transferable visual models from natural language supervision. In: International conference on machine learning. pp. 8748–8763. PmLR (2021)
25. Ren, Z., Pan, Y., Chen, J., Zhao, L., Liao, M., Qian, X., Gong, W.: A survey on deep learning-based chinese font style transfer. IEEE Transactions on Artificial Intelligence (2025)
26. Rezende, D.J., Mohamed, S., Wierstra, D.: Stochastic backpropagation and approximate inference in deep generative models. In: Proceedings of the 31st International Conference on Machine Learning (ICML). pp. 1278–1286 (2014)
27. Rombach, R., Blattmann, A., Lorenz, D., Esser, P., Ommer, B.: High-resolution image synthesis with latent diffusion models. In: Proceedings of the IEEE/CVF conference on computer vision and pattern recognition. pp. 10684–10695 (2022)
28. Ronneberger, O., Fischer, P., Brox, T.: U-net: Convolutional networks for biomedical image segmentation. In: Medical image computing and computer-assisted intervention–MICCAI 2015: 18th international conference, Munich, Germany, October 5–9, 2015, proceedings, part III 18. pp. 234–241. Springer (2015)
29. Ruiz, N., Li, Y., Jampani, V., Pritch, Y., Rubinstein, M., Aberman, K.: Dreambooth: Fine tuning text-to-image diffusion models for subject-driven generation. In: Proceedings of the IEEE/CVF conference on computer vision and pattern recognition. pp. 22500–22510 (2023)
30. Saharia, C., Ho, J., Chan, W., Salimans, T., Fleet, D.J., Norouzi, M.: Image super-resolution via iterative refinement. IEEE transactions on pattern analysis and machine intelligence **45**(4), 4713–4726 (2022)
31. Simonyan, K., Zisserman, A.: Very deep convolutional networks for large-scale image recognition. arXiv preprint arXiv:1409.1556 (2014)
32. Song, J., Meng, C., Ermon, S.: Denoising diffusion implicit models. In: International Conference on Learning Representations (2021)
33. Song, Y., Ermon, S.: Generative modeling by estimating gradients of the data distribution. Advances in neural information processing systems **32** (2019)

34. Standardization Administration of China: Code of chinese graphic character set for information interchange—primary set. GB 2312-1980 (National Standard of the People’s Republic of China) (1980)
35. Standardization Administration of China: Information technology—chinese coded character set. GB 18030-2022 (National Standard of the People’s Republic of China) (2022)
36. Sun, D., Ren, T., Li, C., Su, H., Zhu, J.: Learning to write stylized chinese characters by reading a handful of examples. In: Proceedings of the Twenty-Seventh International Joint Conference on Artificial Intelligence. pp. 920–927. International Joint Conferences on Artificial Intelligence Organization (2018)
37. Tang, L., Cai, Y., Liu, J., Hong, Z., Gong, M., Fan, M., Han, J., Liu, J., Ding, E., Wang, J.: Few-shot font generation by learning fine-grained local styles. In: Proceedings of the IEEE/CVF conference on computer vision and pattern recognition. pp. 7895–7904 (2022)
38. Van Den Oord, A., Vinyals, O., et al.: Neural discrete representation learning. *Advances in neural information processing systems* **30** (2017)
39. Vaswani, A., Shazeer, N., Parmar, N., Uszkoreit, J., Jones, L., Gomez, A.N., Kaiser, Ł., Polosukhin, I.: Attention is all you need. *Advances in neural information processing systems* **30** (2017)
40. Wang, L., Liu, Y., Sharum, M.Y., Yaako, R.B., Kasmiranm, K.A., Wang, C.: Deep learning for chinese font generation: A survey. *Expert Systems with Applications* p. 127105 (2025)
41. Wang, Z., Bovik, A.C., Sheikh, H.R., Simoncelli, E.P.: Image quality assessment: from error visibility to structural similarity. *IEEE transactions on image processing* **13**(4), 600–612 (2004)
42. Yang, A., Pan, J., Lin, J., Men, R., Zhang, Y., Zhou, J., Zhou, C.: Chinese clip: Contrastive vision-language pretraining in chinese. *arXiv preprint arXiv:2211.01335* (2022)
43. Yang, Z., Peng, D., Kong, Y., Zhang, Y., Yao, C., Jin, L.: Fontdiffuser: One-shot font generation via denoising diffusion with multi-scale content aggregation and style contrastive learning. In: Proceedings of the AAAI conference on artificial intelligence. vol. 38, pp. 6603–6611 (2024)
44. Zhang, R., Isola, P., Efros, A.A., Shechtman, E., Wang, O.: The unreasonable effectiveness of deep features as a perceptual metric. In: Proceedings of the IEEE conference on computer vision and pattern recognition. pp. 586–595 (2018)
45. Zhang, Y., Zhang, Y., Cai, W.: A unified framework for generalizable style transfer: Style and content separation. *IEEE Transactions on Image Processing* **29**, 4085–4098 (2020)